Acta Physiologica

Acta Physiol 2009, **195**, 101–110

REVIEW

Measuring diffusion parameters in the brain: comparing the real-time iontophoretic method and diffusion-weighted magnetic resonance

I. Vorisek and E. Sykova

Institute of Experimental Medicine, Academy of Sciences of the Czech Republic, and Department of Neuroscience, Charles University, Prague, Czech Republic

Received 18 June 2008,
accepted 9 September 2008
Correspondence: E. Sykova,
Department of Neuroscience,
Institute of Experimental Medicine,
ASCR, v.v.i., Vídeňská 1083, 142
20 Prague 4, Czech Republic.
E-mail: sykova@biomed.cas.cz

Abstract

The extracellular space (ECS) diffusion parameters influence the movement of ions, neuroactive substances, hormones and metabolites in the nervous tissue. They also affect extrasynaptic transmission, a mode of signal transmission dependent solely on diffusion. This review compares in detail two methods for studying diffusion in the brain: the real-time iontophoretic tetramethylammonium method for ECS volume fraction and tortuosity measurements and diffusion weighted-magnetic resonance imaging for measuring the apparent diffusion coefficient of water. The results obtained using both methods under physiological conditions (post-natal development, ageing) or in pathologies (brain injury, ischaemia) and their similarities and differences are discussed.

Keywords apparent diffusion coefficient, diffusion anisotropy, extracellular matrix, extracellular space, extrasynaptic transmission, tortuosity, volume fraction.

The extracellular space (ECS) represents the microenvironment of nerve cells and is essential for the delivery of oxygen and glucose from the vascular system to brain cells (Nicholson 2001). This microenvironment also serves as a communication channel (Nicholson & Phillips 1979, Sykova 1992) for extrasynaptic transmission among neurones, axons and glia (Fuxe & Agnati 1991, Zoli *et al.* 1999, Nicholson & Sykova 1998, Sykova 2004a,b). This mode of communication is essential for long-range information processing in functions such as hunger, sleep, vigilance, depression, chronic pain, synaptic plasticity and memory formation (Sykova 1997, 2001). The functions of glial cells in the nervous tissue are manifold, including the formation of the blood–brain barrier, trophic support, developmental functions, control of extracellular pH and ionic homeostasis and the electrical insulation of axons. Whereas for neurones signal transmission through the ECS is an alternative mode of communication, for glial cells diffusion in the ECS represents their only communication channel. This fact emphasizes the importance of the ECS diffusion properties for signal reception by glia and, especially, for neurone–glia interactions (Sykova 2005). Diffusion in the ECS is also important for synaptic transmission and for neuronal excitability as well. The ensheathing of synapses by glial processes and by the extracellular matrix (ECM) can not only prevent the spread of neurotransmitters away from a synapse, thus affecting receptors on other synapses (a phenomenon known as synaptic crosstalk), but can also regulate the speed and efficiency of neurotransmitter re-uptake. Neurotransmitters are rapidly cleared from the area for recycling by specialized membrane proteins in the pre- or post-synaptic membrane. This re-uptake prevents desensitization of the post-synaptic receptors and ensures that succeeding action potentials will elicit the same size of excitatory post-synaptic potential. The diffusion parameters in the vicinity of the synaptic cleft may play an important role in this process. The perineuronal nets (Celio *et al.* 1998) that form diffusion barriers around some neurones can affect their excitability. Gurevicius *et al.* (2004) reported enhanced

 doi: 10.1111/j.1748-1716.2008.01924.x

cortical and hippocampal neuronal excitability in mice deficient in the extracellular matrix glycoprotein tenascin-R. This proteoglycan is an important constituent of the perineuronal nets surrounding parvalbumin-positive, inhibitory interneurones. Sykova (2005a) reported that tenascin-R-deficient mice have a much smaller ECS size than do control animals. The movement of substances in the ECS is ensured by diffusion, and thus it is important to study the diffusion properties of tissue. The ECS volume in the nervous tissue and viscosity in the ECS microenvironment change under physiological as well as pathological conditions (Sykova 2004b), affect the movement of substances in the ECS and can contribute to disease progression or the deterioration of cognitive abilities (Sykova *et al.* 2002, Sykova & Nicholson 2008).

Extracellular space diffusion parameters: how to quantify the properties of the extracellular space?

Steady-state diffusion in a homogeneous medium is described by Fick's first law:

$$J = -D\nabla C, \tag{1}$$

where J is the diffusion flux, ∇C is the concentration gradient and D is the diffusion coefficient, which is proportional to the velocity of the diffusing particles. D depends on the temperature and viscosity of the medium and the size of the particles. The diffusion of compounds in the brain ECS differs from diffusion in a homogeneous, infinite medium. The cell membranes and ECM molecules constitute a barrier to the movement of ions and molecules, therefore diffusion in the nervous tissue is restricted (Le Bihan & Basser 1995). While in an infinite medium 100% of the space is available for diffusion, diffusion in the ECS is limited by its size. For a quantitative description of the size of the ECS, the concept of the extracellular volume fraction (α) was introduced (Nicholson & Phillips 1981):

$$\alpha = \frac{V_{ECS}}{V_{TOT}}, \tag{2}$$

where V_{ECS} is the volume of the ECS and V_{TOT} is the total tissue volume. Fick's first law can be used to describe diffusion in the ECS; however, a new parameter, D^*, the effective diffusion coefficient, has to be used:

$$J = -D^*\nabla C. \tag{3}$$

The effective diffusion coefficient is also referred to as the apparent diffusion coefficient (ADC) to emphasize its difference from the diffusion coefficient found in a homogeneous medium. Because of obstacles in the diffusion pathway in the ECS, the displacement of a particle for a given unit of time (and apparent velocity) is smaller than in medium. Note that the real velocity of a particle in the ECS (at the microscopic level) is the same as in medium, but the pathway is more complex, i.e. more tortuous. Therefore, the effective diffusion coefficient in the ECS is always smaller than the diffusion coefficient in medium. The more obstacles in the ECS, the lower is the effective diffusion coefficient. However, the effective diffusion coefficient is not suitable for describing the diffusion properties of the ECS because it is related not only to the properties of the ECS, but also to the specific molecule or ion under study – a molecule of different size has a different diffusion coefficient. The concept of tortuosity (λ) was introduced to overcome this problem:

$$\lambda = \sqrt{\frac{D}{D^*}}. \tag{4}$$

Tortuosity has a simple geometrical interpretation: it expresses the prolongation of the diffusion pathway between two points in the ECS when compared to the diffusion pathway between two points the same distance apart in a homogeneous medium (Fig. 1a,b). The equation 4 tells us how to measure tortuosity; it is sufficient to measure the diffusion coefficient of a molecule or ion in the ESC and in medium. In theory, tortuosity should be independent of the size of the molecule; in the real world, this is true only for molecules with a relative molecular weight up to ~10 000. For larger molecules, whose size is not negligible when compared to the pore size of the ECS, the calculated tortuosity can increase (Prokopova-Kubinova *et al.* 2001) because only small molecules can pass through the small pores, which reduces the number of 'short cuts' in the ESC and thus prolongs the diffusion pathway (Fig. 1c). However, the molecular weights of most neuroactive substances are below this approximate limit. The tortuosity calculated from the effective diffusion coefficient in the ECS and the diffusion coefficient in medium of a single compound of small molecular weight can be used to assess the diffusion of any lightweight molecule or ion in the ECS.

The diffusion coefficient and tortuosity are directionally dependent, as implied by their tensor nature. To fully describe the diffusion properties in a medium, six independent components of the tensor have to be known. In practice, the diffusion coefficient is measured in many directions (at least in six), and the data are used for tensor calculation. As it is complicated to present the diffusion properties of the tissue as a tensor, the concepts of mean diffusivity ($\bar{D}$) and fractional anisotropy (FA) were introduced:

$$\bar{D} = \frac{D_1 + D_2 + D_3}{3}, \tag{5}$$

Journal compilation © 2008 Scandinavian Physiological Society, doi: 10.1111/j.1748-1716.2008.01924.x

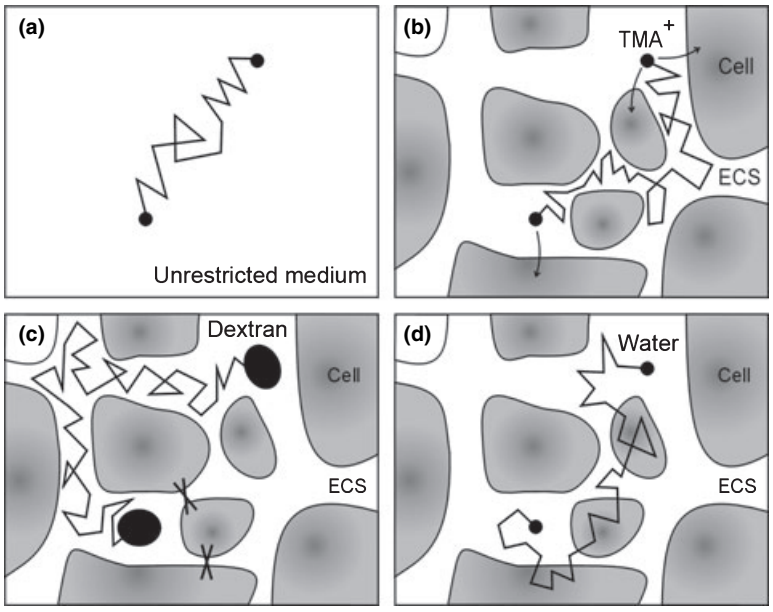

Figure 1 Diffusion of substances in the brain. (a) Free diffusion in an unrestricted medium depends only on the diffusion coefficient and temperature. (b) The cell membrane forms a semi-permeable barrier for diffusion in the extracellular space, and the diffusion of molecules also depends on the size and geometry of the extracellular space. The diffusion of a molecule is slower than in free medium, which is expressed by the concepts of the effective diffusion coefficient D^* and tortuosity. (c) Tortuosity remains constant for small molecules, but it can be increased for very large molecules, as not the entire extracellular space is available for their diffusion. (d) Water is ubiquitous in the brain, therefore measurements of the apparent coefficient of water cover diffusion in multiple compartments.

$$\mathrm{FA} = \sqrt{\frac{2}{3}}\sqrt{\frac{(D_1-\bar{D})^2+(D_2-\bar{D})^2+(D_3-\bar{D})^2}{D_1^2+D_2^2+D_3^2}}, \quad (6)$$

where D_1, D_2 and D_3 are tensor eigenvalues. In the uncomplicated case where $\bar{D} = D_1 = D_2 = D_3$, FA = 0 and the medium is isotropic in relation to diffusion.

In addition, there is one more parameter necessary in order to fully describe the diffusion of ions and molecules in the ECS. Cell membranes, which form barriers to diffusion, can be semi-permeable and thus diffusing compounds can disappear from the ECS by entering into cells. Non-specific uptake (k') is used to describe the speed of clearance of a compound from the ECS.

Methods for measuring the extracellular space parameters and diffusion in the brain

There are only a few methods that allow one to measure the ECS diffusion parameters volume fraction and tortuosity, and in fact there is only one method available to measure all these parameters simultaneously. This is an electrophysiological method that uses ion-selective microelectrodes to determine the changes in the concentration of a detectable compound after injecting it from a point source into the ECS (Nicholson & Sykova 1998, Sykova & Nicholson 2008). Injection via a glass micropipette is done by a pressure pulse or by iontophoresis. This method is unique in its ability to determine the absolute values of α and λ simultaneously. Recently developed methods using a fluorescent probe can measure only tortuosity. The first such method detects changes in the emitted light intensity and its distribution after the injection of a compound labelled by a fluorescent probe (Tao 1999). When using dextrans of different molecular weights, this method is suitable for studying differences in the diffusion of large molecules. The second optical method employs the phenomenon called photobleaching, which is the photochemical destruction of a fluorophore (Binder *et al.* 2004). The fluorophore is destroyed in a small area, which will appear under a fluorescent microscope as a dark spot. The recovery of fluorescence over time is governed by the diffusion coefficient of the fluorescent molecules, which allows the calculation of tortuosity. All the methods mentioned above can be used for measurements *in vitro* as well as *in vivo*. Their common disadvantage is their limited spatial resolution, as the data cannot be acquired from distant areas at the same time; their other drawback is the invasiveness of the measurement procedure.

There are also methods that do not measure the ECS diffusion parameters directly, but which determine a

 doi: 10.1111/j.1748-1716.2008.01924.x

parameter that can be correlated to extracellular volume fraction or tortuosity. These include monitoring the distribution of radioactively labelled material in the tissue (Fenstermacher & Patlak 1977), conductivity measurements (Okada *et al.* 1994), methods based on light scattering in the tissue (Sykova *et al.* 2003) and measurements of the ADC of water using diffusion-weighted magnetic resonance (MR) (Vorisek *et al.* 2002, Sykova 2005a). This last method is the most important because it is non-invasive, provides good spatial resolution and the scanners that can be used for these measurements are widely available. Together, these advantages make MR an important tool for studying diffusion parameters in the brain in clinical research.

Because studies on diffusion in the central nervous system have been primarily performed using one of two methods, we will describe these in more detail and compare them.

Real-time iontophoretic tetramethylammonium method

To measure ECS volume fraction (α) and ECS tortuosity (λ), the real-time iontophoretic method measures the diffusion of a tracer compound (most commonly the tetramethylammonium cation – TMA^+) injected into the ECS by a current pulse. TMA^+ is released by iontophoresis from a microelectrode and its local concentration measured by a TMA-selective microelectrode located about 100–150 μm from the release site. To maintain accurate spacing, both microelectrodes are glued together in a fixed array (Fig. 2a). The concentration–time profiles during and after an iontophoretic pulse (TMA^+ diffusion curves) are recorded and used to determine α and λ (Fig. 2b). In a non-steady state when the concentration of a compound changes with respect to time, diffusion obeys Fick's second law:

$$\frac{\partial C}{\partial t} = D\nabla^2 C, \qquad (7)$$

where ∇^2 is the Laplace operator. A modification of equation 7 can be used to describe the dynamic diffusion-dependent changes in the concentration of a substance injected into the ECS of the brain (Nicholson & Phillips 1981):

$$\frac{\partial C}{\partial t} = \frac{q}{\alpha} + D^*\nabla^2 C, \qquad (8)$$

where q is the source density. By solving equation 8, we can obtain the time course of changes in TMA^+ concentration during and after an iontophoretic pulse. If r is the distance between the tips of the source and ion-selective microelectrodes, $Q = In/F$ (mol s^{-1}) is the iontophoresis source term, where I is the current, typically 100 nA, n is the transport number for TMA^+ and a specific iontophoresis electrode, and F is the Faraday constant, t is the time after starting the iontophoretic pulse, and the time interval $(0, t_p)$ is the duration of the iontophoretic pulse, then the TMA^+ concentration C is given by:

$$C(r,t) = \left(\frac{Q\lambda^2}{8\pi D\alpha r}\right)\left[\exp\left(r\lambda\sqrt{\frac{k'}{D}}\right)\mathrm{erfc}\left(\frac{r\lambda}{2\sqrt{Dt}} + \sqrt{k't}\right) + \exp\left(-r\lambda\sqrt{\frac{k'}{D}}\right)\mathrm{erfc}\left(\frac{r\lambda}{2\sqrt{Dt}} - \sqrt{k't}\right)\right] \quad \text{for } t \leqslant t_p \quad (9)$$

and

$$C'(t) = C(t) - C(t - t_p) \quad \text{for } t > t_p. \qquad (10)$$

Note that despite the relative impermeability of cell membranes to TMA^+, non-specific uptake must be taken into account in equations 9 and 10 in order to obtain the correct results. The equation 9 describes the increase in TMA^+ concentration during a current source pulse; equation 10 is complementary to equation 9 and

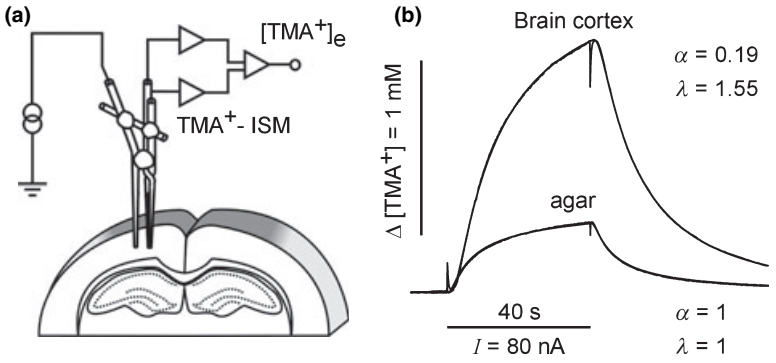

Figure 2 Method for determining the extracellular space volume fraction α and tortuosity λ in the brain *in vivo*. (a) Schematic diagram of the experimental arrangement for diffusion measurements. Two microelectrodes, a double-barrelled TMA^+-selective microelectrode and a micropipette for TMA^+ iontophoresis, are glued together to enable the measurement of TMA^+ diffusion curves (concentration vs. time profiles). (b) TMA^+ diffusion curves were measured with the same microelectrode array in diluted agar and in the mouse brain. Subsequently, the curves were used to calibrate the microelectrode and to calculate α and λ.

Journal compilation © 2008 Scandinavian Physiological Society, doi: 10.1111/j.1748-1716.2008.01924.x

describes the decay in the TMA^+ concentration after the end of the current pulse. Diffusion curves (Fig. 2b) are first recorded in 0.3% agar gel to calibrate the microelectrode array, i.e. to obtain the transport number n (an iontophoresis electrode characteristic) and the array spacing r. The transport number and array spacing can be determined by solving equations 9 and 10 because by definition, in agar the diffusion parameters are $\alpha = 1$, $\lambda = 1$ and $k' = 0$. Subsequently, recordings are done in the brain to obtain the ECS diffusion parameters α, λ and k'. The calculations are done by fitting the diffusion curves to equations 9 and 10.

Diffusion-weighted magnetic resonance

Magnetic resonance is based on the behaviour of nuclei with an odd number of nucleons (e.g. ^1H, ^3He, ^{13}C, ^{17}O, ^{23}Na, ^{31}P) in a magnetic field. Such MR-sensitive nuclei have spin and a related intrinsic magnetic moment. If a sample containing, for example, hydrogen nuclei is placed in a magnetic field, the spins of approximately one-half of the sample nuclei will orient along the magnetic field direction, while the rest will point against the magnetic field direction. The number of spins that are pointed along the magnetic field is slightly higher than the number pointed in the opposite direction because of the lower energy and thus the higher probability of the aligned state. Although the imbalance is very small (a few nuclei per million), it causes the macroscopic magnetization momentum of the sample – net magnetization. The magnetic vector of protons can be broken down into two orthogonal components: a longitudinal component (M_L) and a transverse component (M_T). At equilibrium, when all spins are parallel to the external magnetic field, the transverse component of magnetization is zero. However, the spins of the nuclei in the magnetic field can be deflected from their equilibrium by a radiofrequency pulse at a certain 'resonance' frequency, resulting in changes in both longitudinal and transverse magnetization. The frequency (ω) depends on the type of nuclei and on the strength of the magnetic field (B). Larmor's equation quantifies this dependence:

$$\omega = \gamma B, \tag{11}$$

where γ is the gyromagnetic ratio. When the spins are deflected, they begin to return to equilibrium because of the influence of magnetic inhomogeneities formed by the spin–lattice interaction. The speed of the relaxation of the longitudinal and transverse components of magnetization can be described by T_1 and T_2 relaxation times respectively.

$$M_L = M_L^0\left(1 - \exp\left(\frac{-t}{T_1}\right)\right) \tag{12}$$

$$M_T = M_T^0 \exp\left(\frac{-t}{T_2}\right) \tag{13}$$

where $t = 0$ is the time of the radiofrequency pulse. As the relaxation times are influenced by the lattice and thus by material properties, the relaxation times can distinguish among different tissue types (such as skin, bones, cerebral cortex) and can offer a basis for imaging techniques in biology. According to the type of relaxation time used for imaging, the images are called T_1- or T_2-weighted. In practice, protons are generally used for imaging because of the abundance of hydrogen in living organisms. For diffusion-weighted MR imaging, in addition to a homogenous magnetic field, a pulse of a gradient magnetic field is applied. As the resonance frequency and the precession of the proton spins are dependent on the magnetic field, protons will precess at different rates, resulting in a loss of coherence. Another pulse of the gradient magnetic field in the same direction, but opposite in magnitude, should restore coherence. However, in the interim some protons (hydrogen nuclei in movable water) will have changed their position because of diffusion. These precede at a frequency that does not perfectly match the second gradient pulse, with the result that the loss of coherence cannot be repaired completely, leading to signal loss. The greater the spatial shift of water molecules (i.e. the higher the diffusion coefficient), the greater is the signal loss. The signal (S) decay according to the gradient field strength can be expressed by the following equation:

$$\frac{S}{S_0} = \exp\left(-\gamma^2 G^2 \delta^2 (\Delta - \delta/3) D\right) = \exp(-bD), \tag{14}$$

where S_0 is the signal intensity before gradient magnetic field application, G is the strength of the gradient magnetic field pulse, δ is the duration of the pulse and Δ is the time interval between the first and second gradient pulses. Usually, equation 14 is expressed in a simplified form incorporating a b-factor, which provides information about the strength of the diffusion-weighting. If a tissue is measured repeatedly, each time with different diffusion weighting, then the series of measurement can be used for calculating the ADC of water (ADC_W) by fitting the data to equation 14.

The nature of ADC_W is rather complicated. In contrast to the diffusion of TMA^+, which, if injected into the ECS, stays and diffuses in the ECS, water is present in both the extracellular and intracellular compartments (Fig. 1d). In addition, the diffusion properties in the cytoplasm could differ from those in organelles or in axons. Therefore, ADC_W expresses the averaged contribution of the ADCs from multiple compartments.

Changes in diffusion parameters in health and disease

In the brain, the ECS volume fraction is a stable parameter with a similar value ($\alpha \sim 0.2$) in different brain structures, even in different species (Rice *et al.* 1993, Perez-Pinzon *et al.* 1995, Prokopova-Kubinova & Sykova 2000). The diffusion parameters change during neuronal activity as a result of ionic shifts through neuronal and glial membranes accompanied by water transport (Sykova *et al.* 1992). Small regional differences result in diffusion inhomogeniety (Fig. 4). Using the TMA method, Svoboda & Sykova (1991) detected a transient decrease in ECS volume fraction (of 20–40%) in the spinal dorsal horns of rats after repetitive electrical stimulation of the peripheral nerves. Using diffusion-weighted MR, Darquie *et al.* (2001) observed a transient decrease in the ADC of water (ADC_W) in the human visual cortex during activation by a black and white 8-Hz-flickering checkerboard. Functional MR imaging (fMRI) most often uses changes in BOLD (blood-oxygen-level dependent) signals. In general, BOLD signal is well correlated with changes in the blood flow; however, the exact relationship between the measured fMRI signal and the underlying neural activity is unclear (Logothetis *et al.* 2001). In contrast, changes in ADC_W can be related to ECS volume changes (Darquie *et al.* 2001, Sotak 2004), and thus diffusion-weighted MR makes possible the acquisition of activation maps from the human brain, which are associated directly with neuronal activation.

The ECS size also changes during brain development and ageing (Fig. 3). In the brain cortex of rat pups at a post-natal age of 3–6 days, the ECS volume fraction was 0.43, at 10–12 days 0.27, and at 21–23 days 0.23, while tortuosity remained constant ($\lambda = 1.5$; Vorisek & Sykova 1997a,b). Similarly, a significant decrease was found during post-natal cortical development in the rat by diffusion-weighted MR (Sizonenko *et al.* 2007). It is obvious that a decrease in ADC_W is related to a change in the ECS size. However, if modified, tortuosity can also influence ADC_W. As well as in the grey matter, the ECS volume fraction also decreases post-natally in white matter. Tortuosity increases significantly in the rat corpus callosum between the second and third post-natal weeks when measured in the direction across the nerve fibres (Vorisek & Sykova 1997b). In the incompletely myelinated corpus callosum at post-natal day 4–9, diffusion in the ECS is isotropic. Myelin sheaths at post-natal days 21–23 hinder diffusion across the axons but have a negligible effect on diffusion along the axons. ADC_W is decreased during myelination as well, the decrease being more pronounced in directions across the axons (Chahboune *et al.* 2007). Increased tortuosity contributes to a decrease in ADC_W.

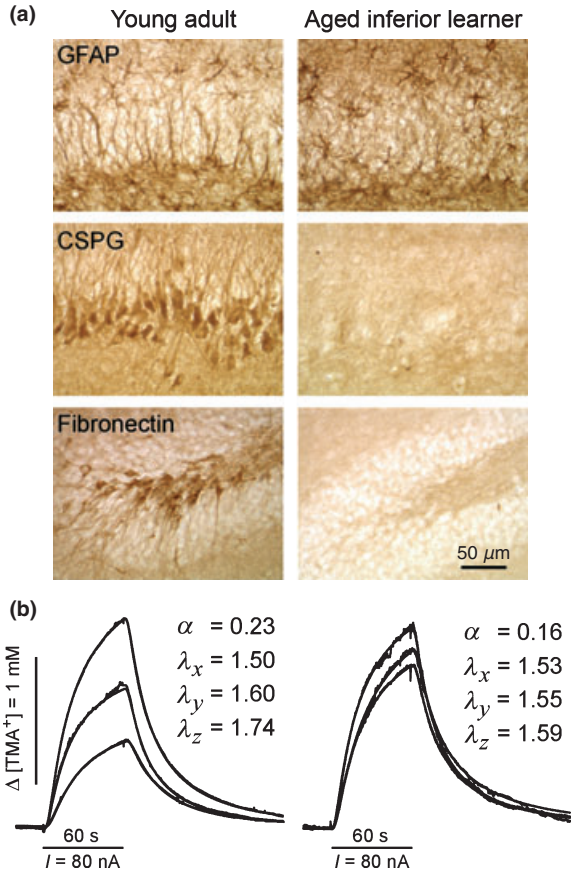

Figure 3 (a) Staining for the astrocyte marker, glial fibrillary acidic protein (GFAP), shows a disruption of the radial organization of astrocytic processes in the dentate gyrus in aged rats, more pronounced in inferior learners. Staining for two components of the extracellular matrix, chondroitin sulphate proteoglycan (CSPG) and fibronectin, reveals a large decrease in the presence of these macromolecules in aged rat brains, especially in the brains of inferior learners. (b) Diffusion curves obtained in the dentate gyrus of aged inferior learners and young adult rats (controls). The diffusion curves acquired along three axes in different directions (*x*: medio-lateral, *y*: rostro-caudal, *z*: dorso-ventral) did not differ greatly in aged rats, demonstrating decreased diffusion anisotropy (i.e. the tortuosity values did not differ) in aged inferior learners. In addition, a smaller extracellular space volume fraction was found in aged rats, when compared to controls.

Because there is a preferential direction for diffusion along the axons in white matter (decreased tortuosity), the tensor measurement of ADC_W and FA analysis can be used to visualize the white matter tracts in the brain and the spinal cord in health and disease. This technique, termed tractography, can reveal developmental abnormalities, changes associated with ageing, neurodegenerative diseases, demyelinating diseases and psychiatric diseases. Moreover, it can visualize anatomic reorganization in ischaemic diseases or in the vicinity of a tumour and can be used in pre-operative

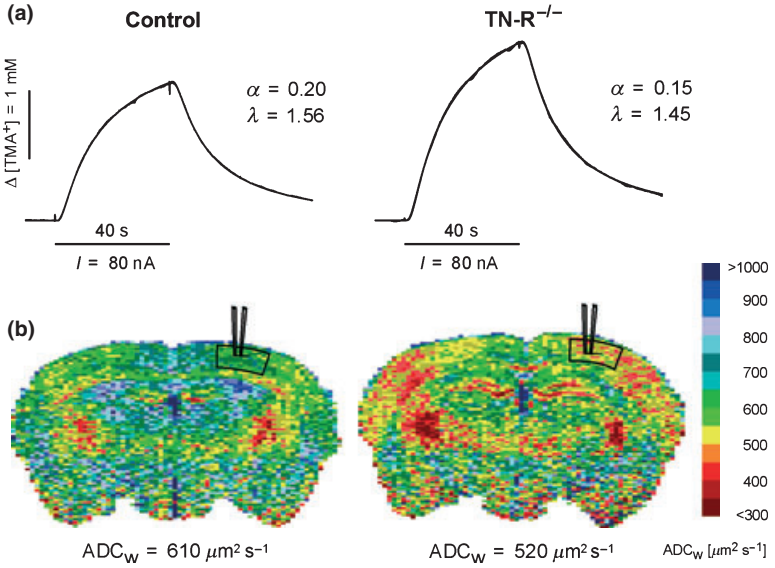

Figure 4 (a) TMA^+ measurements performed in the primary somatosensory cortex. Note that the extracellular space (ECS) volume fraction is lower and the diffusion curve shows a higher amplitude (i.e. a faster rise and fall time) in the TN-$R^{-/-}$ mouse than in the control mouse. (b) ADC_W maps acquired in the brain of control and TN-$R^{-/-}$ mice. The mean value of ADC_W was calculated in the delineated areas (primary somatosensory cortex). The mean values of ADC_W and ECS volume fraction (α) are given below each map. The scale at the right side of the figure shows the relation between the intervals of ADC_W values and the colours used for visualization.

planning for epilepsy surgery. For a review of the clinical applications of tractography, see Nucifora *et al.* (2007). Measurements of diffusion anisotropy can even be correlated with cognitive abilities. Sykova *et al.* (2002) measured tortuosity along different axes in the hippocampus of behaviourally tested aged rats. The rats were separated into two groups on the basis of their performance in a Morris water maze (Morris 1984). The volume fraction was decreased in the hippocampus of inferior learners. Measurements of tortuosity along different axes (parallel to and perpendicular to the astrocytic processes) revealed the loss of diffusion anisotropy in the hippocampus of aged inferior learners. This loss of anisotropy was manifested predominantly by a significant decrease in tortuosity along the dorsoventral axis in inferior learners (λ = 1.64) when compared to both young adult rats and aged superior learners (λ = 1.74). The authors also found histological correlates of the changes in diffusion anisotropy. Staining for fibronectin and chondroitin-sulphate proteoglycan revealed a loss of ECM molecules that form perineuronal nets. Staining for the astrocyte marker glial fibrillary acidic protein showed a disruption in the radial organization of astrocytic processes in the inner blade of the dentate gyrus in aged inferior learners (Fig. 3). The loss of radial organization could affect ECS diffusion anisotropy.

As demonstrated above, the ADC of water reflects changes in both the ECS volume fraction and tortuosity; more specifically, ADC_W correlates positively with α and negatively with λ. In acute ischaemia in the rat cerebral cortex, α rapidly decreases from 0.22 to 0.05 and λ simultaneously increases from 1.5 to 2.2 (Vorisek & Sykova 1997a,b). Both α and λ influence ADC_W to change in the same direction, resulting in a reduction of ADC_W of 50% (Van Der Toorn *et al.* 1996). There have been attempts to find a dependence between ECS volume fraction and tortuosity; in particular, Archie's law has been extensively discussed (Nicholson & Rice 1986, Lundbaek & Hansen 1992, Latour *et al.* 1994). This relation was derived empirically by Archie in 1942 to describe the impedance properties of porous soils:

$$\lambda^2 = \gamma\alpha^{-\beta}, \qquad (15)$$

where γ and β are the empirical parameters. Archie's law can be used to describe the diffusion properties of the ECS only in some limited cases (e.g. in ischaemia). However, equation 15 is not well suited to explain measurements in which α and λ change independently (Kume-Kick *et al.* 2002). Also, other studies devoted to, e.g. post-natal development or X-radiation injury (Sykova *et al.* 1996) reported the independent behaviour of α and λ. In a model of traumatic injury (Vorisek *et al.* 2002), the ECS volume fraction increased in the vicinity of the wound from 0.21 to 0.27, and tortuosity increased from 1.57 to 1.83. In the same area, ADC_W was not significantly different from control values as a consequence of the opposing contributions of α and λ to ADC_W. When the ECS volume fraction increases, ADC_W increases as well, but an increase in tortuosity hinders the diffusion of water in the ECS and therefore is related to a decrease in ADC_W. Tortuosity sometimes conforms to Archie's law, but sometimes it changes independently of alterations in the ECS volume fraction. The probable cause of this phenomenon is the ambiguous origin of tortuosity: it has a geometrical component, which reflects membrane obstacles to diffusion, and a viscous component, which has its origin in large macromolecules (the ECM) posing a hindrance for

 doi: 10.1111/j.1748-1716.2008.01924.x

diffusion (Rusakov & Kullmann 1998). The increase in tortuosity at the wound site is caused not only by a change in the geometry of astrocytic processes, but also primarily by the overexpression of ECM molecules (Vorisek *et al.* 2002), resulting therefore in a large increase in the viscous component of tortuosity.

Alterations in ECM composition also lead to changes in α, as shown in a study conducted using tenascin-R-deficient mice (Sykova 2005a). Tenascin-R-deficient mice show a decrease in the expression not only of tenascin-R, but also of other molecules of the ECM such as, e.g. chondroitin-sulphate proteoglycan. These complex alterations in the ECM content were manifested by a significant decrease in α from 0.20 to 0.15 as well as a decrease in λ from 1.55 to 1.49, when compared to control mice. The decrease in ECS volume fraction was accompanied by a decrease in ADC_W from 580 to 530 $\mu m^2 s^{-1}$ (Fig. 4). A loss of ECM molecules (for example, chondroitin-sulphate proteoglycan or fibronectin) also appears during ageing, resulting in a decrease in both the ECS volume fraction and the ADC of water (Sykova *et al.* 2002, 2005b, Vorisek *et al.* 2008). In contrast, α and ADC_W can increase as a result of the extracellular deposition of amyloid. Sykova *et al.* (2005b) found that a significant increase in the ECS volume fraction and an increase in the ADC of water are closely related to amyloid plaque deposition in APP23 mice, a model of Alzheimer's disease.

Conclusion

The ECS-diffusion parameters, as measured by the real-time iontophoretic TMA method, ECS volume fraction and tortuosity provide important information for experimental and clinical neuroscience research. The methods employed for direct measurement of these parameters are less suitable for clinical use because of their invasiveness. Fortunately, the ADC of water, measured by diffusion-weighted MR, can be correlated to ECS volume fraction and tortuosity. In general, ADC_W increases in correlation with an increase in the ECS volume fraction and vice versa. However, if tortuosity is increasing excessively and simultaneously with a mild increase in the ECS volume fraction, then their combined contribution to a change in ADC_W reflects a cancelling out of their individual contributions. In such a case, diffusion-weighted MR is not able to detect changes in the ECS diffusion parameters. Tensor measurement of ADC_W, which reflects diffusion anisotropy and directionally dependent changes in tortuosity, can be used to detect developmental abnormalities, neurodegenerative diseases and anatomical reorganization. Although diffusion-weighted MR does not provide complete information about the diffusion parameters in the ECS, the ADC_W changes can be better interpreted when correlated with the ECS diffusion parameters measured by the real-time TMA^+ iontophoresis method.

Conflict of interest

The authors have no conflict of interest with regard to the subject matter of this article.

This work was supported by the grants AV0Z50390512 from the Grant Agency of the Academy of Sciences of the Czech Republic and 1M0538 and LC554 from the Ministry of Education, Youth and Sports of the Czech Republic.

References

Binder, D.K., Papadopoulos, M.C., Haggie, P.M. & Verkman, A.S. 2004. In vivo measurement of brain extracellular space diffusion by cortical surface photobleaching. *J Neurosci* **24**, 8049–8056.

Celio, M.R., Spreafico, R., De Biasi, S. & Vitellaro-Zuccarello, L. 1998. Perineuronal nets: past andpresent. *Trends Neurosci* **21**, 510–515.

Chahboune, H., Ment, L.R., Stewart, W.B., Ma, X., Rothman, D.L. & Hyder, F. 2007. Neurodevelopment of C57B/L6 mouse brain assessed by in vivo diffusion tensor imaging. *NMR Biomed* **20**, 375–382.

Darquie, A., Poline, J.B., Poupon, C., Saint-Jalmes, H. & Le Bihan, D. 2001. Transient decrease in water diffusion observed in human occipital cortex during visual stimulation. *Proc Natl Acad Sci USA* **98**, 9391–9395.

Fenstermacher, J.D. & Patlak, C.S. 1977. CNS, CSF, and extradural fluid uptake of various hydrophilic materials in the dogfish. *Am J Physiol Regul Integr Comp Physiol* **232**, 45–53.

Fuxe, K. & Agnati, L.F. 1991. *Volume transmission in the brain: novel mechanisms for neural transmission*. Raven Press, New York.

Gurevicius, K., Gureviciene, I., Valjakka, A., Schachner, M. & Tanila, H. 2004. Enhanced cortical and hippocampal neuronal excitability in mice deficient in the extracellular matrix glycoprotein tenascin-R. *Mol Cell Neurosci* **25**, 515–523.

Kume-Kick, J., Mazel, T., Vorisek, I., Hrabetova, S., Tao, L. & Nicholson, C. 2002. Independence of extracellular tortuosity and volume fraction during osmotic challenge in rat neocortex. *J Physiol* **542**, 515–527.

Latour, L.L., Svoboda, K., Mitra, P.P. & Sotak, C.H. 1994. Time-dependent diffusion of water in a biological model system. *Proc Natl Acad Sci USA* **91**, 1229–1233.

Le Bihan, D. & Basser, P.J. 1995. Molecular diffusion and nuclear magnetic resonance. In: D. Le Bihan & P.J. Basser (eds) *Diffusion and Perfusion Magnetic Resonance Imaging, Applications to Functional MRI*, pp. 5–17. Raven Press, New York.

Logothetis, N.K., Pauls, J., Augath, M., Trinath, T. & Oeltermann, A. 2001. Neurophysiological investigation of the basis of the fMRI signal. *Nature* **412**, 150–157.

Lundbaek, J.A. & Hansen, A.J. 1992. Brain interstitial volume fraction and tortuosity in anoxia. Evaluation of the ion-

Journal compilation © 2008 Scandinavian Physiological Society, doi: 10.1111/j.1748-1716.2008.01924.x

selective micro-electrode method. *Acta Physiol Scand* **146**, 473–484.

Morris, R. 1984. Developments of a water-maze procedure for studying spatial learning in the rat. *J Neurosci Methods* **11**, 47–60.

Nicholson, C. 2001. Diffusion and related transport mechanisms in brain tissue. *Rep Prog Phys* **64**, 815–884.

Nicholson, C. & Phillips, J.M. 1979. Diffusion of anions and cations in the extracellular microenvironment of the brain. *J Physiol* **296**, 66p.

Nicholson, C. & Phillips, J.M. 1981. Ion diffusion modified by tortuosity and volume fraction in the extracellular microenvironment of the rat cerebellum. *J Physiol (Lond)* **321**, 225–257.

Nicholson, C. & Rice, M.E. 1986. The migration of substances in the neuronal microenvironment. *Ann N Y Acad Sci* **481**, 55–71.

Nicholson, C. & Sykova, E. 1998. Extracellular space structure revealed by diffusion analysis. *Trends Neurosci* **21**, 207–215.

Nucifora, P.G., Verma, R., Lee, S.K. & Melhem, E.R. 2007. Diffusion-tensor MR imaging and tractography: exploring brain microstructure and connectivity. *Radiology* **245**, 367–384.

Okada, Y.C., Huang, J.C., Rice, M.E., Tranchina, D. & Nicholson, C. 1994. Origin of the apparent tissue conductivity in the molecular and granular layers of the *in vitro* turtle cerebellum and the interpretation of current source-density analysis. *J Neurophysiol* **72**, 742–753.

Perez-Pinzon, M.A., Tao, L. & Nicholson, C. 1995. Extracellular potassium, volume fraction, and tortuosity in rat hippocampal CA1, CA3, and cortical slices during ischemia. *J Neurophysiol* **74**, 565–573.

Prokopova-Kubinova, S. & Sykova, E. 2000. Extracellular diffusion parameters in spinal cord and filum terminale of the frog. *J Neurosci Res* **62**, 530–538.

Prokopova-Kubinova, S., Vargova, L., Tao, L., Ulbrich, K., Subr, V., Sykova, E. & Nicholson, C. 2001. Poly[N-(2-hydroxypropyl) methacrylamide] polymers diffuse in brain extracellular space with same tortuosity as small molecules. *Biophys J* **80**, 542–548.

Rice, M.E., Okada, Y.C. & Nicholson, C. 1993. Anisotropic and heterogeneous diffusion in the turtle cerebellum: implications for volume transmission. *J Neurophysiol* **70**, 2035–2044.

Rusakov, D.A. & Kullmann, D.M. 1998. Geometric and viscous components of the tortuosity of the extracellular space in the brain. *Proc Natl Acad Sci USA* **95**, 8975–8980.

Sizonenko, S.V., Camm, E.J., Garbow, J.R., Maier, S.E., Inder, T.E., Williams, C.E., Neil, J.J. & Huppi, P.S. 2007. Developmental changes and injury induced disruption of the radial organization of the cortex in the immature rat brain revealed by in vivo diffusion tensor MRI. *Cereb Cortex* **17**, 2609–2617.

Sotak, C.H. 2004. Nuclear magnetic resonance (NMR) measurement of the apparent diffusion coefficient (ADC)of tissue water and its relationship to cell volume changes in pathological states. *Neurochem Int* **45**, 569–582.

Svoboda, J. & Sykova, E. 1991. Extracellular space volume changes in the rat spinal cord produced by nerve stimulation and peripheral injury. *Brain Res* **560**, 216–224.

Sykova, E. 1992. *Ionic and Volume Changes in the Microenvironment of Nerve and Receptor Cells*. Springer-Verlag, Berlin.

Sykova, E. 1997. The extracellular space in the CNS: Its regulation, volume and geometry in normal and pathological neuronal function. *Neuroscientist* **3**, 28–41.

Sykova, E. 2001. Glial diffusion barriers during aging and pathological states. *Prog Brain Res* **132**, 339–363.

Sykova, E. 2004a. Extrasynaptic volume transmission and diffusion parameters of the extracellular space. *Neuroscience* **129**, 861–876.

Sykova, E. 2004b. Diffusion properties of the brain in health and disease. *Neurochem Int* **45**, 453–466.

Sykova, E. 2005. Glia and volume transmission during physiological and pathological states. *J Neural Transm* **112**, 137–147.

Sykova, E. & Nicholson, C. 2008. Diffusion in brain extracellular space. *Physiol Rev*. (in press).

Sykova, E., Svoboda, J., Simonova, Z. & Jendelova, P. 1992. Role of astrocytes in ionic and volume homeostasis in spinal cord during development and injury. *Prog Brain Res* **94**, 47–56.

Sykova, E., Svoboda, J., Simonova, Z., Lehmenkühler, A. & Lassmann, H. 1996. X-irradiation-induced changes in the diffusion parameters of the developing rat brain. *Neuroscience* **70**, 597–612.

Sykova, E., Mazel, T., Hasenohrl, R.U., Harvey, A.R., Simonova, Z., Mulders, W.H.A.M. & Huston, J.P. 2002. Learning deficits in aged rats related to decrease in extracellular volume and loss of difussion anisotropy in hippocampus. *Hippocampus* **12**, 469–479.

Sykova, E., Vargova, L., Kubinova, S., Jendelova, P. & Chvatal, A. 2003. The relationship between changes in intrinsic optical signals and cell swelling in rat spinal cord slices. *NeuroImage* **18**, 214–230.

Sykova, E., Vorisek, I., Mazel, T., Antonova, T. & Schachner, M. 2005a. Reduced extracellular space in the brain of tenascin-R- and HNK-1-sulphotransferase deficient mice. *Eur J Neurosci* **22**, 1873–1880.

Sykova, E., Vorisek, I., Antonova, T., Mazel, T., Meyer-Luehman, M., Jucker, M., Hajek, M., Ort, M. & Bures, J. 2005b. Changes in extracellular space size and geometry in APP23 transgenic mice - a model of Alzheimer's disease. *Proc Natl Acad Sci USA*, **102**, 479–484.

Tao, L. 1999. Effects of osmotic stress on dextran diffusion in rat neocortex studied with integrative optical imaging. *J Neurophysiol* **81**, 2501–2507.

Van Der Toorn, A., Sykova, E., Dijkhuizen, R.M., Vorisek, I., Vargova, L., Skobisova, E., Van Lookeren Campagne, M., Reese, T. & Nicolay, K. 1996. Dynamic changes in water ADC, energy metabolism, extracellular space volume, and tortuosity in neonatal rat brain during global ischemia. *Magn Res Med* **36**, 52–60.

Vorisek, I. & Sykova, E. 1997a. Ischemia-induced changes in the extracellular space diffusion parameters, K^+ and pH in

the developing rat cortex and corpus callosum. *J Cereb Blood Flow Metab* **17**, 191–203.

Vorisek, I. & Sykova, E. 1997b. Evolution of anisotropic diffusion in the developing rat corpus callosum. *J Neurophysiol* **78**, 912–919.

Vorisek, I., Hajek, M., Tintera, J., Nicolay, K. & Sykova, E. 2002. Water ADC, extracellular space volume and tortuosity in the rat cortex after traumatic injury. *Magn Reson Med* **48**, 994–1003.

Vorisek, I., Jirak, D., Namestkova, K., Hajek, M. & Sykova, E. 2008. Decreased mean diffusivity and changes in proton spectra in the brain of aged rats with learning deficits. *Proc Intl Soc Mag Reson Med* **16**, 813.

Zoli, M., Jansson, A., Syková, E., Agnati, L.F. & Fuxe, K. 1999. Intercellular communication in the central nervous system: the emergence of the volume transmission concept and its relevance for neuropsychopharmacology. *Trends Pharmacol Sci* **20**, 142–150.

 doi: 10.1111/j.1748-1716.2008.01924.x